

# The Macroscopic Limit in a Stochastic Reaction–Diffusion–Process

Heinz–Peter Breuer, Wolfgang Huber and Francesco Petruccione  
*Albert-Ludwigs-Universität, Fakultät für Physik,  
 Hermann-Herder-Straße 3, D-79104 Freiburg im Breisgau,  
 Federal Republic of Germany*

## Abstract

*Extensive numerical simulation of a reaction–diffusion–system reveal an unusual system size dependence of the fluctuation magnitude. If  $\Omega$  denotes the system size parameter, e.g. particle number, fluctuations are usually predicted to be of order  $\Omega^{0.5}$  (stable case) or  $\Omega^1$  (diffusion–type case). In contrast, a scaling like  $\Omega^{0.84}$  is observed in a combined birth–death and random–walk process, which is described by a multivariate chemical master equation and corresponds to the Fisher equation in the macroscopic limit.*

**PACS:** 05.40.+j; 87.10.+e; 82.20.-w

**The system.** In this work we consider the following simple nonlinear reaction–diffusion–system: Particles are distributed along one spatial coordinate and move by way of diffusion. They react according to the scheme  $A \rightleftharpoons 2A$ . Thus, the presence of  $A$ -particles at some location leads to further production, and at the same time reactions of two  $A$ -particles will destroy one of them.

**Macroscopic Description.** Mean field theory yields a deterministic reaction–diffusion equation by completely neglecting the fluctuations. In the present case, this is the *Fisher equation*. It is a nonlinear partial differential equation for the space and time dependent concentration variable  $c(x, t)$ :

$$\frac{\partial c}{\partial t} = \gamma \frac{\partial^2 c}{\partial x^2} + c - c^2 \quad . \quad (1)$$

Here,  $\gamma$  is the (space- and time–independent) diffusion coefficient, and both reaction rates have been absorbed by choosing appropriate units for  $x$  and  $t$ . Equation (1) was proposed by Fisher to model the spread of advantageous genes [1] and its relevance stems from the fact that it admits stable travelling wave solutions.

The typical situation of interest is the one in which a front is moving to the right, replacing the unstable  $c = 0$  state by the stable  $c = 1$  state. There are front solutions for any front velocity. However, there is a velocity selection principle which guarantees that, for localized initial conditions (i. e.  $c(x, 0) = 0$  for  $x \geq x_0$ ), the front velocity approaches the asymptotic value  $v_F = 2\sqrt{\gamma}$ . The Fisher equation is usually studied as a prototype to understand the qualitative properties of waves or bifurcations in more complicated processes [2–6].

**Mesoscopic Description.** The mesoscopic master equation description of distributed reacting systems takes into account the effects of internal fluctuations, which are caused by the underlying microscopic dynamics of the discrete particles [7, 8]. Position space is divided into  $M$  intervals or cells, such that the particle distribution in each cell is homogeneous. The state of the system is given by the set of positive, integer-valued particle numbers  $\{N_\lambda \mid \lambda = 1, \dots, M\}$ . This many-particle representation is analogous to the second quantization in quantum mechanics. The diffusive motion of the particles is described as a collective random walk between the cells, and reactions within the cells are modelled as a birth and death process.

The present analysis is neither restricted to the diffusion-controlled nor to the reaction-controlled limit. The latter case is included by considering only one single cell; in the diffusion-controlled limit the number  $M$  of cells is large, and the occupation numbers  $N_\lambda$  are either 0 or 1. Here, we consider systems where the density is so high that there may be many particles in one cell. The typical cell occupation number is expressed by the parameter  $\Omega$ . In our simulations,  $\Omega$  ranged from  $10$  to  $10^5$ .

The mesoscopic, stochastic model is completely contained in the many-particle master equation. Together with an initial condition it uniquely determines the time-dependent joint probability distribution  $P(N_1, \dots, N_M, t)$ :

$$\begin{aligned} \frac{d}{dt}P = & \sum_{\lambda=1}^M \frac{\gamma}{\Omega^2} (\mathbf{E}_{\lambda-1}^{-1} \mathbf{E}_\lambda + \mathbf{E}_{\lambda+1}^{-1} \mathbf{E}_\lambda - \mathbf{2}) N_\lambda P \\ & + \sum_{\lambda=1}^M \left( (\mathbf{E}_\lambda^{-1} - \mathbf{1}) N_\lambda + (\mathbf{E}_\lambda - \mathbf{1}) \frac{1}{\Omega} N_\lambda (N_\lambda - 1) \right) P . \end{aligned} \quad (2)$$

The shift operator  $\mathbf{E}_\lambda^{\pm 1}$  changes every  $N_\lambda$  to the right of it by  $\pm 1$ . The first line of equation (2) corresponds to diffusive or random walk transitions, the second line to reactive transitions. Equation (2) is discussed in detail in reference [9]. Microscopic lattice simulations of Fisher-like systems and exact results are reported in references [10-13], Boltzmann equation simulations can be found in reference [14].

**Statement of the Problem.** What is the relation between the macroscopic and the mesoscopic level of description? For many systems, it is possible to show

that in a certain limit, which we shall call *macroscopic limit*, the expectation values of the stochastic process described by the master equation are governed by the macroscopic equation. Higher moments then simply lead to small fluctuations around the deterministic path. Our numerical analysis will show that and why this is not the case for the system under consideration, and we shall deduce a power-law for the scaling of the fluctuations with the system size.

**The macroscopic limit.** For equation (2) the macroscopic limit is given by

$$\begin{aligned} \Omega &\rightarrow \infty \\ \tilde{\gamma} := \gamma/\Omega^2 &= \text{const.} \end{aligned} \quad . \quad (3)$$

The parameter  $\Omega$  is the mean particle number per cell in the stable stationary state behind the front. The width of the front is controlled by  $\gamma$ . Namely,  $\sqrt{\gamma}$  is proportional to its width measured in units of  $x$ , and  $\sqrt{\tilde{\gamma}}$  is proportional to the number of cells within the front. Furthermore, as is read off the master equation,  $\tilde{\gamma}$  is proportional to the ratio of the frequency of diffusion events to that of the reaction events.

**Numerical results.** The master equation was numerically solved by means of a stochastic simulation algorithm [15] which generates a sample of realizations of the stochastic process. This was done for a wide range of parameters  $\Omega$  and  $\tilde{\gamma}$ . For each parameter selection, around 50 realizations were generated, and the simulation time corresponds to 5–100 autocorrelation times of the slowest mode. The spatial extent  $M$  of the grid was large enough that no particle reached the right boundary during this time; on the left side, particles were reflected. Details are described in reference [9].

The solid lines in Figure 1 show, at the same time, seven different realizations which emerged from a step initial condition. For comparison, the dashed line shows an approximation of the stable  $v_F = 2\sqrt{\gamma}$  wave front solution of the macroscopic Fisher equation at an arbitrary horizontal position [5]. While the mean front position of the ensemble wanders to the right with a given mean speed, the individual realizations themselves may be slower or faster and thus their horizontal positions differ. This is caused by translatable fluctuations, i.e. by perturbations that displace the whole front along the  $\lambda$ -axis. Since the master equation is, just as the Fisher equation, translationally invariant, such fluctuations are not at all damped. The deterministic drift of the front to the right is superposed with a Brownian motion.

Let us define a quantitative measure for the front position. It is measured as the area under the graph defined by the front:

$$N_{tot}(t) = \sum_{\lambda=\lambda_1}^{\infty} N_{\lambda}(t) \quad . \quad (4)$$

Here,  $\lambda_1$  is an arbitrary reference cell to the left of the front. The front velocity  $v_M$  can now be defined as the time derivative of the ensemble average  $\langle N_{tot}(t) \rangle$ . In reference [9] we reported numerical results for the stationary value of  $v_M$  after relaxation for a large range of parameters. We observed a surprising difference between  $v_M$  and the value  $v_F = 2\sqrt{\gamma}$  even for large system-size of the stochastic system, i. e. even for large values of  $\Omega$ .

The ensemble variance of  $N_{tot}$  is a measure for the size of the fluctuations of the front position.  $\text{Var}(N_{tot})$  is the variance estimator

$$\text{Var}(N_{tot}) = \frac{1}{n-1} \sum_{i=1}^n (N_{tot}^{(i)} - \bar{N}_{tot})^2 \quad . \quad (5)$$

Figure 2 shows its growth with time. The sample comprises  $n = 60$  realizations with parameter values of  $\Omega = 100$  and  $\tilde{\gamma} = 10$ . We see that  $\text{Var}(N_{tot})$ , after a certain relaxation time of approximately 10 units, grows linearly with time. This is of course reminiscent of a diffusion process, with the diffusion coefficient  $D$  estimated as

$$D = \frac{\text{Var}(N_{tot})|_{t=t_b} - \text{Var}(N_{tot})|_{t=t_a}}{t_b - t_a} \quad . \quad (6)$$

In Figure 2, we have  $t_a = 20$ ,  $t_b = 59.5$  and  $D = 744000$ . In this manner  $D$  was determined for a large range of parameter values. The results are presented in the double-logarithmic plot depicted in Figure 3. Within statistical errors, the data are fitted by straight lines. Note that  $\Omega$  varies over four decades. A least square linear regression yields a slope of  $1.68 \pm 0.03$  for the solid line ( $\tilde{\gamma} = 1$ ) and consistent values for the other two lines. Consequently, the numerical data are very well fitted through a power law of the form

$$D = \Omega^{2\alpha} f(\tilde{\gamma}) \quad (7)$$

with

$$\alpha = 0.84 \pm 0.02 \quad .$$

We can now summarize the behaviour of the probability distribution of the front position  $N_{tot}$ . Starting with an ensemble of identically prepared systems, the mean  $\langle N_{tot} \rangle$  has a certain initial value and the variance is zero. After relaxation, the mean  $\langle N_{tot} \rangle$  grows linearly with time, leading to a front speed of approximately  $2\Omega\sqrt{\tilde{\gamma}}$ , and this value is expected to become exact in the macroscopic limit. Moreover, also the variance  $\text{Var}(N_{tot})$  grows linearly with time according to equation (6). The distribution of  $N_{tot}$  can be seen to remain unimodal and approximately Gaussian for all times. The relative spread of the front position is given by the dimensionless quantity

$$\frac{\sqrt{\text{Var}(N_{tot})}}{\langle N_{tot} \rangle} \approx \frac{\sqrt{Dt}}{v_M t} \propto \frac{\sqrt{\Omega^{2\alpha}}}{\sqrt{t}\Omega} = \frac{1}{\sqrt{t}} \Omega^{\alpha-1} \quad . \quad (8)$$

The expression on the right hand side is obtained by combining equations (6) and (7) and using  $\langle N_{tot} \rangle = v_M t$ .

There are two conclusions to be drawn from equation (8): (i) Since  $\alpha \approx 0.84$  is smaller than one, the relative spread of the front position vanishes in the macroscopic limit (3). We also know that the fluctuations of the front form are damped, as is illustrated in Figure 1 and shown explicitly in references [5, 9]. Thus the dynamic of the front becomes deterministic in the macroscopic limit. (ii) The approach to this limit, as measured by the relative spread of the front position, is approximately proportional to  $\Omega^{-0.16}$ , and therefore extraordinarily slow.

**Discussion.** In many cases, it is possible in the macroscopic limit to split up the stochastic dynamics defined by a master equation into a deterministic and a small stochastic part [7, 16]. A systematic procedure is the  $\Omega$ -expansion which uses the ansatz  $N_\lambda = \Omega c_\lambda + \Omega^{0.5} \eta_\lambda$ . Here,  $N_\lambda$  are the extensive stochastic variables indexed by  $\lambda$ ,  $\Omega$  is the system-size parameter and  $c_\lambda$  are intensive deterministic functions which may be identified with the expectation values  $\langle N_\lambda \rangle / \Omega$ . To leading order an equation for the  $c_\lambda$  is obtained. If its linearization is asymptotically stable, the expansion converges and the equation for the transformed stochastic variables  $\eta_\lambda$  becomes independent of  $\Omega$  in the limit  $\Omega \rightarrow \infty$ . This implies that the relative spread, as defined in equation (8), of  $N_\lambda$  or any linear function thereof is of order  $\Omega^{-0.5}$ .

If one naively applies the  $\Omega$ -expansion formalism to the master equation (2), one obtains the (discrete space) Fisher equation as the macroscopic equation. However, the necessary stability criterion is violated: The wave front solutions are not stable to translative perturbations, as we have seen above. Consequently, the relative spread of the front position scales approximately as  $\Omega^{-0.16}$  and vanishes much slower for  $\Omega \rightarrow \infty$  as in cases where the  $\Omega$ -expansion applies.

One might now perhaps presume that the Fisher-like system is, because of its zero-mode, of the “diffusion-type” [7]. However, for diffusion-type systems there is no nontrivial macroscopic equation and the relative spread of the variables scales as  $\Omega^0$ , i. e. does not vanish for  $\Omega \rightarrow \infty$ . This clearly does not accord with our numerical results, which indicate that there is a nontrivial macroscopic deterministic equation (the Fisher equation), and that the relative spread vanishes.

The validity of a macroscopic equation in describing a real reaction-diffusion-system always depends on the system being close enough to the macroscopic limit. For the present Fisher-like system, we conclude that this limit in principle exists but point out that there will be many real systems which are far away from that limit. Recall that the relative spread (8) vanishes as slowly as  $\Omega^{-0.16}$ . For such finite systems, fluctuations are not negligible and may have, as reported earlier [9], a significant influence on the dynamics of the mean values. We expect

these conclusions not only to apply to the specific system (2), but to a general class of spatially extended systems with a zero-mode of the macroscopic equation.

## References

- [1] R. A. Fisher. *Annals of Eugenics*, VII: 355–369, 1937.
- [2] A. Kolmogorov, I. Petrovsky and N. Piscounov. *Bulleten' Moskovskogo Gosudarstvennogo Universiteta, Sekcija A Matematika i mechanika*, 1: 1–26, 1937.
- [3] D. G. Aronson and H. F. Weinberger. In *Partial Differential Equations and Related Topics*, Vol. 446 of *Lecture Notes in Mathematics*. Springer, New York, 1975.
- [4] Wim van Saarloos. *Physical Review A*, 37: 211–226, 1988.
- [5] J. D. Murray. *Mathematical Biology*. Biomathematics, 19. Springer-Verlag Berlin Heidelberg, 1989.
- [6] M. S. Benilov. *Physics Letters A*, 169: 57–61, 1992.
- [7] N. G. van Kampen. *Stochastic processes in physics and chemistry*. Elsevier Science Publishers B.V., 2nd edition, 1992.
- [8] D. T. Gillespie. *Physica A*, 188: 404–425, 1992.
- [9] H. P. Breuer, W. Huber and F. Petruccione. *Physica D*, 73: 259–273, 1994.
- [10] W. Horsthemke, C. R. Doering, T. S. Ray and M. A. Burschka. *Phys. Rev. A*, 45: 5492–5503, 1992.
- [11] M. Bramson, P. Calderoni, A. De Masi, P. Ferrari, J. Lebowitz and R. H. Schonman. *J. Stat. Phys.*, 45: 905–920, 1986.
- [12] D. ben Avraham, F. Leyvraz and S. Redner. *Phys. Rev. E*, 50: 1843–1850, 1994.
- [13] A. R. Kerstein. *Journal of Statistical Physics*, 45: 921–931, 1986.
- [14] A. Lemarchand, H. Lemarchand, E. Sulpice and M. Mareschal. *Physica A*, 188: 277–283, 1992.
- [15] D. T. Gillespie. *Markov Processes*. Academic Press Inc., San Diego, 1992.
- [16] M. Malek-Mansour, C. van den Broeck, G. Nicolis and J. W. Turner. *Annals of Physics*, 131: 283–313, 1981.

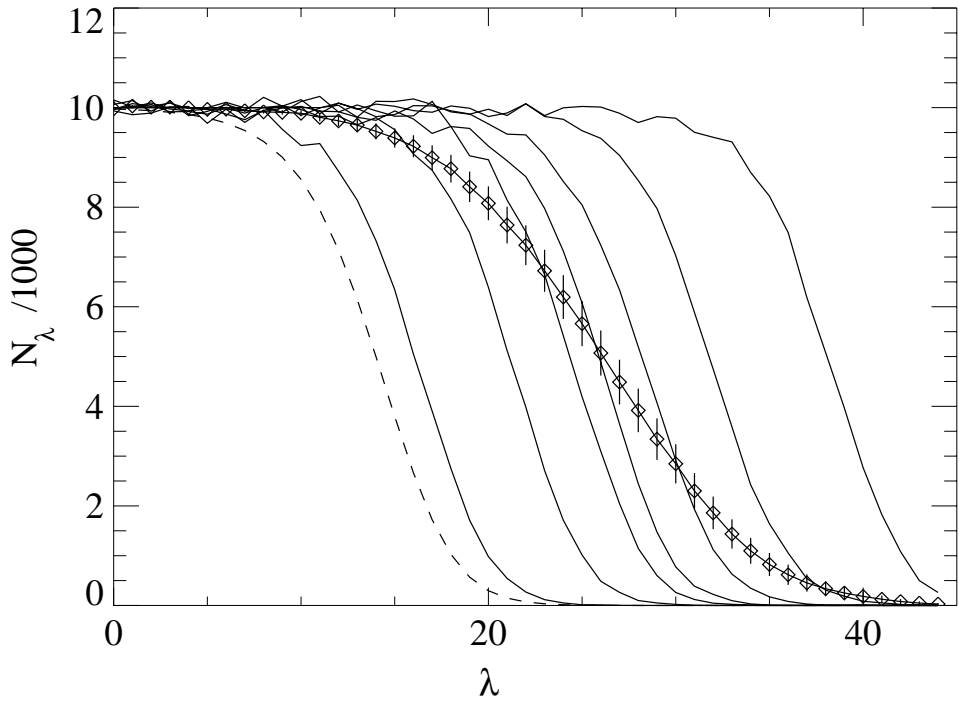


Figure 1: The solid lines show 7 different realizations at the same time  $t = 435$ , for parameter values  $\Omega = 10^4$  and  $\gamma = 10^8$ . The symbols with the error bars denote the mean of 66 realizations and its standard error. For comparison, the dashed line shows an approximation of the stable wave front solution of the Fisher equation.

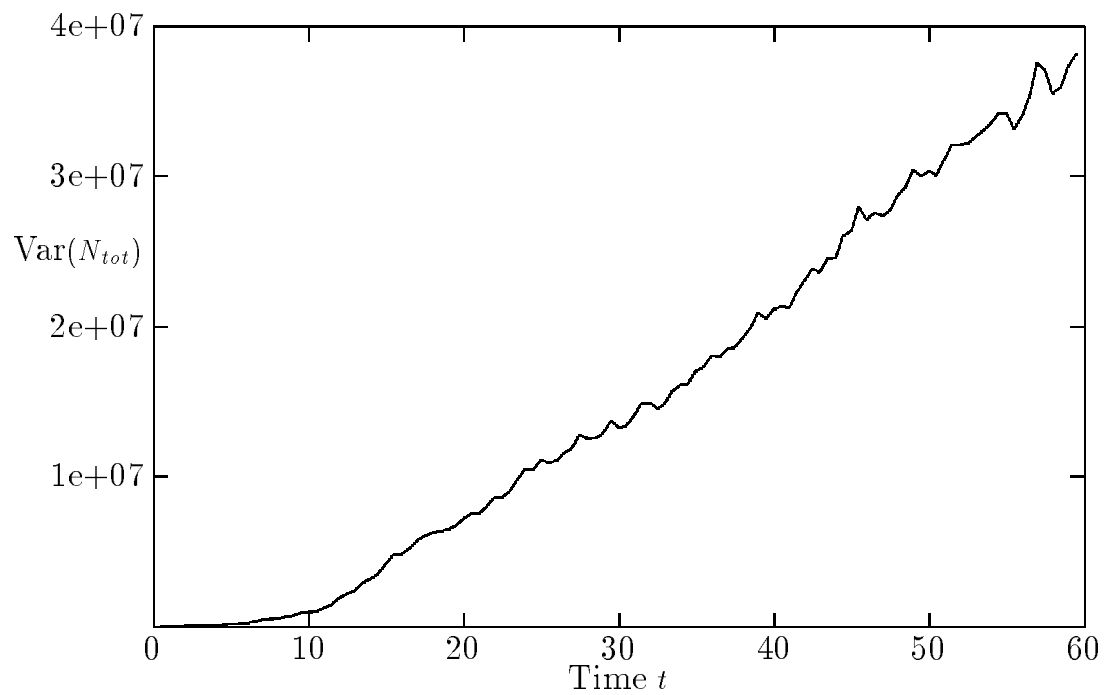


Figure 2: The time-dependence of the variance of the front position  $N_{tot}$ . Parameters are  $\Omega = 1000$ ,  $\tilde{\gamma} = 10$ , sample size: 60 realizations.

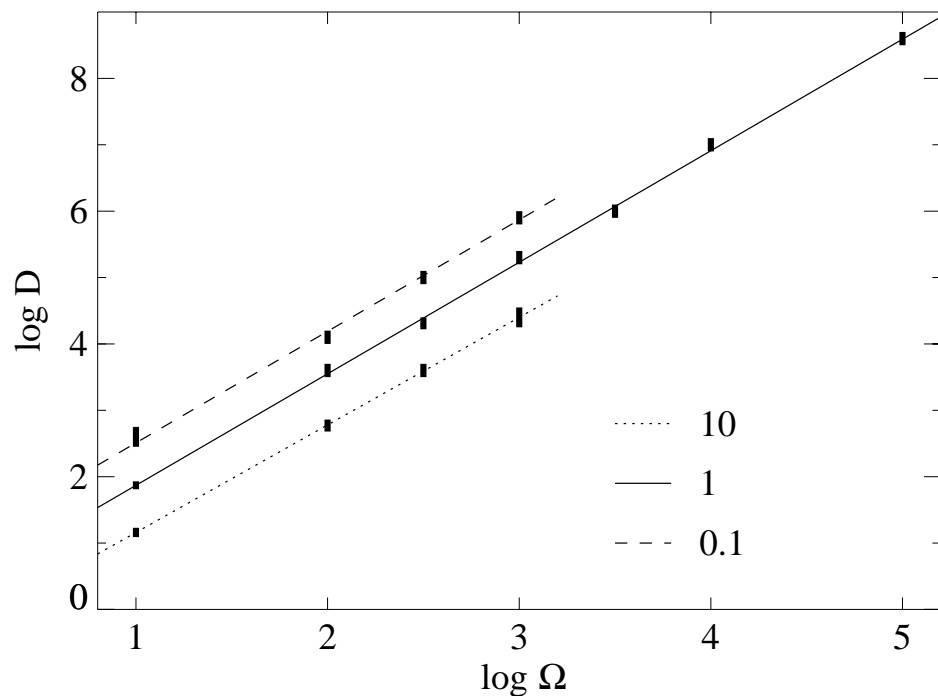


Figure 3: Overview over the numerically found values of  $D$ , defined in equation (6), as a function of  $\Omega$ , for three different values of  $\tilde{\gamma} = 0.1, 1, 10$ .